Physica Medica 66 (2019) 55–65

Contents lists available at ScienceDirect

Physica Medica

journal homepage: www.elsevier.com/locate/ejmp

Original paper

Optimal tumour control for early-stage non-small-cell lung cancer: A radiobiological modelling perspective

Mohammed Alaswad[a,b,*], Christoph Kleefeld[a], Mark Foley[a]

[a] School of Physics, National University of Ireland Galway, Galway, Ireland
[b] Comprehensive Cancer Centre, Radiation Oncology, King Fahad Medical City, Riyadh 11525, Saudi Arabia

ARTICLE INFO

Keywords:
NSCLC
TCP
Clonogenic cell density distribution
GTV–CTV margin

ABSTRACT

A fully heterogeneous population tumour control probability (TCP) model, based on the linear-quadratic (LQ) cell survival concept combined with the Poisson statistic, was established to predict local tumour control after one, two and three years. This TCP model was created using data from 16 publications that reported on early-stage non–small-cell lung cancer (NSCLC) treated using either three-dimensional conformal radiation therapy (3D-CRT), continuous hyperfractionated accelerated radiotherapy (CHART) or stereotactic ablative body radiotherapy (SABR). The TCP model was fitted to the clinical outcome data using optimised radiosensitivity values produced by the Nelder-Mead simplex algorithm. The statistical analysis resulted in R^2 values of 0.96, 0.96 and 0.97 and wRMSE values of 3.9%, 5.2% and 5.9% for one-, two- and three-year local tumour control rates, respectively. The TCP models for one, two and three years were internally validated using a bootstrap resampling approach. The mean R^2 and 95% CI for the bootstrap samples were 0.98 (0.93–0.99), 0.98 (0.95–0.99) and 0.98 (0.96–0.99) for the one-, two- and three-year local tumour control rates, respectively. Variations in the TCP with clonogenic density were then further investigated by introducing a new mathematical model to vary the clonogenic cell and radiation dose distribution across the treated volume. Based on the above model, it was estimated that 60% of the dose was sufficient to maintain the TCP after two years for the areas with lower clonogenic cell density. If externally validated, this lower-dose treatment plan could have beneficial effects on the surrounding healthy tissue without negatively affecting tumour control.

1. Introduction

Lung cancer remains the most common cause of cancer mortality, with approximately 1.81 million patients diagnosed with the disease in 2012 [1]. The two main categories of lung cancer are non–small-cell lung cancer (NSCLC), which includes 80% of all lung cancers, and small-cell lung cancer (SCLC), which accounts for the remaining 20% [2]. Radical surgery remains a treatment mainstay for early-stage NSCLC; however, many patients with NSCLC are not candidates for surgery due to comorbidities, such as cardiopulmonary dysfunction, stage I, II or chronic obstructive pulmonary disease or tumour size during stages III and IV [3], or because they refuse surgery altogether. Consequently, curative external-beam radiotherapy is commonly regarded as an alternative therapeutic procedure for early-stage NSCLC [4].

The conventional fractionation (CF) radiotherapy schedule, as proposed by the Radiation Therapy Oncology Group (RTOG) [5], is 45–70 Gy and includes one treatment per day of 1.8–2.5 Gy per fraction over 6–8 weeks. Notably, CF radiotherapy has historically been associated with poor local tumour control (35%, 17% and 9% at one-, two- and three-year follow-ups, respectively) [6]. Another fractionation scheme suggested by some institutions in the United Kingdom is continuous hyperfractionated accelerated radiotherapy (CHART), which prescribes radiation doses of 54 Gy via 1.5 Gy per fraction delivered 3 times per day. In the United Kingdom, CHART is recommended as the standard of care for patients undergoing a radiotherapy course for NSCLC [7]. This fractionation scheme has the potential to improve local tumour control up to 66%, 40% and 20% at one-, two- and three-year follow-ups, respectively [7].

In addition, improved survival and local tumour control can be attained using stereotactic ablative radiotherapy (SABR), a state-of-the-art technique that is considered the optimal treatment for patients with early-stage NSCLC for whom surgical procedures are not appropriate. Several studies and prospective phase II trials have confirmed that the

* Corresponding author at: School of Physics, National University of Ireland Galway, Galway, Ireland and Comprehensive Cancer Centre, Radiation Oncology, King Fahad Medical City, Riyadh, Saudi Arabia.
E-mail address: medphy00@gmail.com (M. Alaswad).

https://doi.org/10.1016/j.ejmp.2019.09.074
Received 1 July 2019; Received in revised form 6 September 2019; Accepted 8 September 2019
Available online 24 September 2019

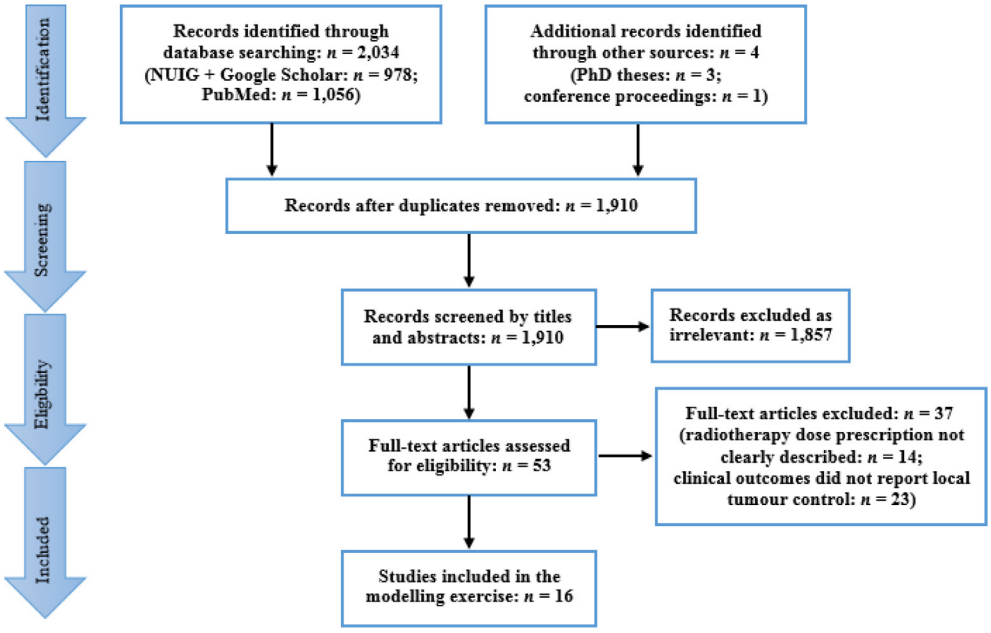

Fig. 1. PRISMA flow diagram illustrating the various phases of the systematic review search and the study selection process.

rates of local tumour control are as high as 83–96% [8–13], significantly higher than the data reported for three-dimensional conformal radiation therapy (3D-CRT) and CHART. SABR is typically performed at a much greater dose per fraction than either 3D-CRT or CHART, and it has generated outstanding local tumour control in early-stage NSCLC (96%, 89% and 84% at one-, two- and three-year follow-ups, respectively) [8]. The authors of the RTOG 0236 research study recommended that SABR can be regarded as the main therapeutic procedure for patients with early-stage NSCLC [6], and it can be argued that SABR is also preferable to surgery for most patients with early-stage NSCLC.

However, from a radiobiology perspective, the application of the linear-quadratic (LQ) concept at such a high dose per fraction is controversial. Considerable debate exists in the literature regarding the accuracy of LQ-based tumour control probability (TCP) modelling for predicting the clinical outcomes encountered at high dose-per-fraction, such as for SABR treatment of NSCLC. For instance, Kirkpatrick et al. argued that the LQ model, which expresses the mechanism of the radiation's interaction with and destruction of DNA, and therefore represents a fundamental component of the TCP model, may be inapplicable to radiation therapy protocols that employ a high dose per fraction [14]. A few authors have defended this view by stating that the eradication of tumours using hypofractionated radiotherapy protocols is determined by biological concepts (e.g., vascular and stromal damage) that are more qualitatively complex than those encountered with standard or hyperfractionated radiotherapy protocols. Therefore, these biological phenomena are not accounted for by the LQ model [15–17]. Similar arguments were made by Park et al., who indicated that radiotherapy treatment courses that apply doses of more than 8.0 Gy/fraction are likely to produce significant vascular damage and injury to the intratumoural microenvironment, thereby leading to indirect tumour cell death [18]; notably, this is not the case for the standard treatment of 2 Gy/fraction. In response, SABR proponents have argued that its efficacy is due to escalated tumour radiation doses that confer high local tumour control and that its toxicity is limited by the same biological phenomena established for lower radiotherapy fractionation schemes, such as those used for CHART and 3D-CRT; therefore, no new radiobiological concepts are required to describe SABR's clinical outcomes [19,20].

The number of clonogens in the tumours of interest is a fundamental input parameter for TCP modelling. Clonogenic cell density for solid tumours can vary widely, ranging from 10^5–10^9 cm^{-3} [21]. The exact value of this number for different tumour types is not known, nor is it understood how this number varies between tumours in different patients. Within this context, various radiobiological methods have been developed and introduced to calculate TCP [22–27]. However, much of this radiobiological research has assumed that the treated volume contains a fixed number of clonogenic cells, which is perceived as one of the major limitations of these models. Notably, a few researchers have indicated that the likelihood of clonogenic cell density decreases from the centre of the gross tumour volume (GTV) towards the edge and that these decreases also occur within the clinical target volume (CTV) [28,29]. In these situations, lower clonogenic cell densities can be destroyed with a relatively lower radiation dose than is usually required to eliminate tumours, while a higher radiation dose would be required to eliminate a tumour with a higher clonogenic cell density. Following these plans, the optimal TCP and normal tissue complication probabilities can be attained.

The objectives of this study were fivefold: (1) to explore the accuracy of a mechanistic TCP model to describe the clinical outcomes of a broad spectrum of NSCLC fractionation schemes, such as standard fractionation, hyperfractionation and hypofractionation; (2) to determine whether SABR's tumouricidal mechanisms are the same as those of 3D-CRT and CHART; (3) to examine the association between radiation dose size and TCP for NSCLCs; (4) to develop a new radiobiological approach for modelling clonogenic density, addressing the current limitations of TCP research in the literature by using a new mathematical approach; and (5) to introduce the concept of a GTV–CTV margin into the TCP model.

2. Methodology

2.1. Patient eligibility

TCP models were fitted to a list of early-stage NSCLC patient data collected from the literature. To identify studies that described clinical outcomes of early-stage NSCLC, a systematic review analysis was conducted using Google Scholar, PubMed and the National University of Ireland Galway academic library databases (see Fig. 1). This systematic review was conducted using the Preferred Reporting Items for

Systematic Reviews and Meta-Analyses (PRISMA) guidelines [30]. The search included papers that had been published or accepted for publication or that appeared as meeting abstracts between June 1989 and September 2018. The full articles were accessed when their abstracts were deemed pertinent. The bibliographies of relevant publications were also explored to locate additional related studies. From each article, detailed clinical outcome information was extracted for model analysis and simulation; this information included the number of patients, the total dose, the number of fractions, the dose per fraction, the radiotherapy modality, the prescription dose and local tumour control. Further inclusion criteria were that patients had to have been treated using one of three external-beam radiation therapy approaches: 3D-CRT, SABR or CHART. The studies also had to report local tumour control details at one-, two- and three-year follow-ups. These inclusion criteria had previously been utilised in radiobiological modelling research conducted by Alaswad et al. [31].

In the first phase of the systematic review, 2034 published articles were identified across the three electronic databases, of which 1910 remained after eliminating all duplicates. EndNote X8.2 software (Thomson Reuters, USA) was used to manage and sort the articles. The article titles and abstracts were then comprehensively screened for the inclusion criteria; 1857 studies were determined to be ineligible, leaving 53 articles that were relevant to the research question. After assessing these full-length articles, 16 studies containing a total of 2713 patients met the inclusion criteria. Articles were excluded for several reasons, including but not limited to imprecise descriptions of radiotherapy dosages or the lack of a detailed quantitative presentation of clinical outcomes. A PRISMA flow chart detailing the process of study identification, inclusion and exclusion is shown in Fig. 1. Table 1 summarises patient dosimetric characteristics and clinical outcomes.

2.2. Model description

Several methods of modelling local tumour control have been previously introduced [24,35]. One of the most popular is the LQ model combined with Poisson statistics, which proposes that local tumour control is only attained if no clonogens survive the delivered radiation dose. The LQ model in Eq. (1) describes the surviving fraction of clonogenic cells, *S(D)*, after exposure to a specific radiation dose *D*. This model has two essential features: (1) a linear component corresponding to nonrepairable single lesions produced by a single track of radiation; and (2) a quadratic component, which is produced by two separate radiation tracks, corresponding to double lesions that are repairable at low doses. The LQ model is mathematically defined by the following equation:

$$\mathbf{S(D) = exp[-\alpha nd \ - \beta nd^2]} \quad (1)$$

where S represents the surviving fraction, n is the number of fraction, d is the dose per fraction, D is the total dose delivered over the treatment course and α (Gy^{-1}) and β (Gy^{-2}) are the intrinsic radiosensitivity factors determining the initial slope and degree of curvature, respectively, of the fundamental cell survival curve.

It is also necessary to include the effects of incomplete sublethal lesion repair when establishing a radiobiological model to predict local tumour control. This has been addressed by introducing an additional factor (h) into Eq. (1). Thames examined the effect of sublethal lesion repair for a fractionated treatment and recommended that the modelling process employ the following formula [36]:

$$\mathbf{h} = \left(\frac{2}{\mathbf{m}}\right)\left(\frac{\theta}{1-\theta}\right)\left(\mathbf{m} - \frac{1-\theta^{\mathbf{m}}}{1-\theta}\right) \quad (2)$$

where m is the number of fractions per day, $\theta = [-\tau\Delta T]$, τ is the repair half-time and ΔT is the time between fractions. Accordingly, Eq. (1) can be rewritten as:

$$\mathbf{S(D) = exp[-\alpha nd \ - \beta n(1+h)d^2]} \quad (3)$$

Clonogenic tumour cells can repopulate during the course of fractionated radiotherapy, thereby reducing treatment effectiveness. This effect may be incorporated into the LQ model by introducing a repopulation correction factor that depends on two main parameters: the treatment duration and the clonogenic doubling time. Accordingly, Eq. (3) can be rewritten as:

$$\boldsymbol{S\ (D) = e^{-n(\alpha d + G\beta^2)+\gamma(T_0 - T_{del})}} \quad (4)$$

where $T_0$is the overall radiation treatment time, T_{del} is the delay time up to the onset of accelerated proliferation and γ is the accelerated repopulation time factor. The γ factor used in this study was $0.693/T_{pot}$, with T_{pot} being the potential doubling time. The values of T_{del} and T_{pot} were 28 days and 5 days, respectively, which are consistent with the observed clinical data reported by Mehta et al. [37,38].

The idea of local tumour control evolved from an assumption that tumour control could only be attained if no clonogens survived after the radiation dose was delivered. TCP is defined by Eq. (5), in which N_0 is the inceptive clonogen number and $S(D)$ represents LQ cell survival:

$$\mathbf{TCP = exp[(-N_0 S(D))]} \quad (5)$$

These TCP models were revised to include a normal distribution of the radiosensitivity parameters α, β, σ_α and σ_β for a particular population utilising a cumulative density function, which allowed the model to be determined for a Gaussian-distributed range of radiosensitivities [23,31,39]. The TCP models make two assumptions: 1) that the radiosensitivity components α and β are distributed normally with standard deviations σ_α and σ_β; and 2) that the components are independent among the lung tumours that comprise the population

Table 1
Published data on 2713 patients with early-stage NSCLC treated by 3D-CRT, CHART or SABR, including their local tumour control rates.

RT modality	Patient cohorts	Ref #	# of patients	d/fraction (Gy)	# of fractions	1-year tumour control (%)	2-year tumour control (%)	3-year tumour control (%)
3D-CRT	1	[32]	225	2.0	30	35.0	13.0	7.0
3D-CRT	2	[6]	203	2.0	33	35.0	17.0	9.0
3D-CRT	3	[33]	104	2.0	35	70.0	40.0	31.0
3D-CRT	4	[34]	56	2.1	32	44.0	34.0	29.0
3D-CRT	5	[34]	32	2.1	38	73.0	47.0	35.0
3D-CRT	6	[34]	18	2.1	46	76.0	50.0	49.0
CHART	7	[7]	849	1.5	36	66.0	40.0	20.0
CHART	8	[3]	23	1.5	36	65.3	39.0	20.0
CHART	9	[6]	203	1.5	40	73.0	43.0	27.0
CHART	10	[4]	583	1.5	36	63.0	31.0	20.0
SABR	11	[9]	92	9.0	5	89.0	83.0	83.0
SABR	12	[10]	38	10.0	5	95.0	93.0	93.0
SABR	13	[8]	128	12.0	5	96.0	89.0	84.0
SABR	14	[11]	40	14.0	3	90.0	88.0	85.0
SABR	15	[12]	88	15.0	3	95.0	89.0	87.0
SABR	16	[13]	31	20.0	3	95.0	84.8	83.8

described by the following equation:

$$\mathbf{TCP} = \frac{1}{2\pi\sigma_\alpha\sigma_\beta}\iint (\exp[-\mathbf{N_0 S(D)}]) \times \exp\left[\frac{-(\alpha-\bar{\alpha})^2}{2\sigma_{\alpha^2}} - \frac{(\beta-\bar{\beta})^2}{2\sigma_{\beta^2}}\right]\mathbf{d}\alpha\mathbf{d}\beta \quad (6)$$

However, this integral can be estimated only through numerical methods and cannot be evaluated analytically; therefore, the present study used the following approach:

$$TCP = \left(\frac{1}{K}\right)\sum_{i=1}^{k}(exp[(-N_0 S(D)_i)]) \quad (7)$$

where K represents a patient cluster with a distinctive radiosensitivity.

Since the model was analytically intractable and the standard fitting methods were inappropriate, the TCP models were, therefore, fitted by employing the Nelder-Mead (NM) simplex algorithm [40]. The NM simplex algorithm is a derivative-free approach used in nonlinear continuous optimisation problems that provides a robust approach in determining a function's local minimum with various variables [41]. With respect to the TCP model in this study, the variables are α, β, $\sigma\alpha$ and $\sigma\beta$. Several initial estimates based on the known plausible ranges of radiosensitivity were used for the model simulations. These initial guesses were based on the radiosensitivity ranges that have been previously reported in the literature [42–44].

In the NM simplex algorithm, the simplex consists of a polyhedron within $n + 1$ vertices of the n-dimensional search space—that is, the number of points (vertices) is equal to one more than the number of dimensions in the search space. For four variables (α, β, $\sigma\alpha$ and $\sigma\beta$), a simplex consists of a pentachoron with a pattern search comparing function values at the five points of the pentachoron. In each iteration, the highest objective function value (known as the worst vertex) is removed and substituted with a new vertex (known as the best vertex). This procedure produces a series of pentachorons with the function values at the points decreasing continuously. The iterations are repeated to minimise the objective function through reflection, expansion, shrinkage and contraction. By iterating this procedure, the NM simplex algorithm determines the best solution.

Accordingly, this algorithm was used to minimise the mean squared error (MSE) that was yielded by the TCP model, which was weighted statistically to the number of patients for each dataset to avoid bias. The optimum TCP fit is that which produces the highest weighted coefficient of determination (R^2) and the lowest weighted mean squared error (wMSE).

In this part of the model, the GTV was considered to have a uniform clonogenic cell distribution. Furthermore, the clonogenic density was set to a value of 10^7 cm^{-3},which was determined to be appropriate based on the clinical data regarding NSCLC [12]. Eq. (8) was used to calculate the initial number of clonogens as proposed by Webb and Nahum [45]:

$$\mathbf{N_0} = \mathbf{GTV} \times \mathrm{P_{clonogens}} \quad (8)$$

In addition, GTV volumes can vary between cancer stages and even between individuals in the same stage [32]. For the selected 3D-CRT and CHART studies (Table 1), the majority of the patients were diagnosed with stage II or III NSCLC. Among these, one phase I randomised trial compared the clinical outcomes of patients diagnosed with stage II and III NSCLC who were treated with either 3D-CRT or CHART; it reported a mean GTV of 85 cm^3 [3]. Accordingly, a mean GTV of 85 cm^3 was used in the present study as the input tumour size parameter for the TCP simulation for patients receiving either CHART or 3D-CRT. However, the included studies that used SABR primarily focused on stage I NSCLC with a mean GTV of 45 cm^3; this value was, therefore, used as the input tumour size parameter for the SABR TCP model in the present study (Table 1).

Cancer cells' response to ionising radiation depends strongly on oxygen, which mediates the indirect influences of ionising radiation and causes cell death; cells become more radioresistant under hypoxic conditions. This hypoxic effect was incorporated into the LQ model using an oxygen enhancement ratio (OER)—i.e., the ratio of doses needed to produce the same biological effect for hypoxic and oxic conditions:

$$S = \exp\left(-\frac{\alpha}{OER}d - \frac{\beta}{OER^2}d^2\right) \quad (9)$$

Within this context, the radiosensitivity parameters α and β depend on partial oxygen pressure, as determined by the OER. Typically, a tumour's OER value is 1.75; however, it has been reported as 2.8 for NSCLCs [14]. Furthermore, research has established the proportion of clonogens defined as hypoxic and oxic to be 20% and 80%, respectively [46], and this was also incorporated into the model.

2.3. Modelling clonogenic cell density

Two computational radiobiological models were developed in MATLAB to study the effects of varying clonogenic density distributions on local tumour control. To the best of our knowledge, no previous study has attempted to model this effect using the new approach described in sections 2.3.1 and 2.3.2. The same 16 patient cohorts described in Table 1 were used to study the effects of clonogenic cell density variations on TCP. Since the central goal of this part of the study was to determine the effect of different clonogenic cell densities on TCPs, only two-year tumour control data were selected to model this effect. These proposed approaches are described in the following subsections.

2.3.1. Modelling clonogenic density decay in the GTV–CTV margin

This first approach sought to investigate a realistic scenario in which the clonogenic cell density inside the GTV remained constant but decreased within the GTV–CTV margins [16,17]. This approach assumed that the entire GTV had a constant and uniform clonogenic cell density of 10^7 cm^{-3} [13–15]. However, the CTV was set to have a clonogenic cell density equal to 10^7 cm^{-3} at the inner edge, decaying to 10^0 cm^{-3} at the outer edge, following a Gaussian distribution (see Eq. (10)).

$$y = \sum_{i=1}^{n} N_{0i} e^{\left[-\left(\frac{r-b_i}{c_i}\right)^2\right]} \quad (10)$$

Here, N_0 is the clonogenic cell density, b is the centroid (location) and c is the decay peak width of the Gaussian decay distribution. The values used for N_0, b and c were 10^7 cm^{-3}, 0 and 0.9, respectively. In addition, r was the range of values (3.0–3.5 cm) that represented the GTV–CTV margin and that determined the fall-off of clonogenic cell density within the GTV–CTV margin.

For this approach, $n = 40$ segments were used, and additional geometric information about the value of the GTV–CTV margin was coded into the computational model, which was considered to be 5 mm, as illustrated in Fig. 2A [24]. The dose per fraction was also varied in the same manner as clonogenic cell density to determine the value for each segment. For instance, the prescribed radiation dose was held constant inside the GTV to match the constant clonogenic cell density and then decreased throughout the GTV–CTV margin, following the Gaussian decay (see Fig. 2A). Eq. (10) was also modified slightly to model the decay of the dose distribution:

$$y = \sum_{i=1}^{n} d_i e^{\left[-\left(\frac{r-b_i}{c_i}\right)^2\right]} \quad (11)$$

where d is the dose per fraction and r determines the radiation dose fall-off within the GTV–CTV margin. The values of the Gaussian parameters b and c were 0 and 5, respectively.

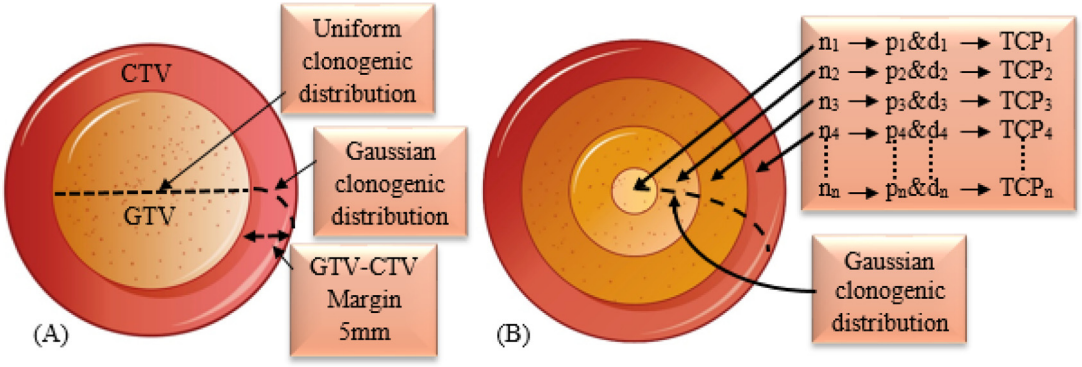

Fig. 2. Proposed methods for modelling clonogenic cell density. (A) Illustrates the clonogenic cell density variations across the GTV and CTV. This model also introduces the concept of the GTV–CTV margin into the TCP. (B) Displays how the model functions as a numerical approximation for a nonuniform clonogenic cell density distribution and nonuniform dose-per-fraction distribution.

2.3.2. Modelling clonogenic density decay across whole-tumour volume

The second approach modelled a half-Gaussian clonogenic distribution from the centre of the GTV. This approach did not attempt to replicate a tumour in a practical sense; rather, its focus was solely on the computational model, and it sought to investigate the sensitivity of varying both the doses and clonogenic cell densities and their interactions in local tumour control by using both Eqs. (10) and (11).

The goal was to deliver a high radiation dose to areas of high clonogenic cell density and a low radiation dose to areas of low clonogenic cell density—in other words, to maximise the dose delivered to high densities and minimise the radiation to low densities. Additional geometric information (such as GTV–CTV margins) was no longer required since the distribution functions would alter clonogenic cell density, and hence, the dose per fraction across all segments, as displayed in Fig. 2B.

2.4. Internal validation

A bootstrap resampling approach was employed to internally validate and verify the robustness of the TCP models. This approach assumed that an appropriate new dataset using the same population could be generated by randomly sampling the initial dataset and combining it with a 'replicate' bootstrap dataset. The points to be used were selected 'with replacement', indicating that a specific point could be selected repeatedly or not at all for a particular bootstrap sample [47]. The internal validation procedure was performed by randomly generating 2000 bootstrap samples; each sample consisted of 16 data points, which were selected with replacement. Both R^2 and RMSE were estimated using bootstrap resampling, with their 95% confidence intervals (CIs) then determined with bias-corrected and accelerated (BCa) percentile intervals.

3. Results

3.1. Prediction of clinical outcomes: LQ-based statistical TCP model

The TCP models expressed a strong positive linear relationship between the literature's reported local tumour control and the estimated TCP outcomes. Fig. 3A, B and C show the correlation coefficient R^2 of statistical tests between the estimated TCPs corresponding to each radiotherapy modality listed in Table 1 (3D-CRT, CHART and SABR). The statistical analysis resulted in tumour control rates of $R^2 = 0.96$ and wRMSE = 3.9% at the first-year follow-up, $R^2 = 0.96$ and wRMSE = 5.2% at the second-year follow-up and $R^2 = 0.97$ and wRMSE = 5.9% at the third-year follow-up; all p-values were < 0.05.

Table 2 summarises the model's predictions of the TCPs for one-year, two-year and three-year local tumour control rates. For patients who received SABR, TCPs were as high as 98.0%, 95.9% and 93.0% at one-, two- and three-year local tumour control rates, respectively, with a biologically effective dose (BED) of ≥ 85.5 Gy. In contrast, the best TCPs for patients in the CHART subgroup were 83.5%, 44.1% and 28.5% at the first-, second- and third-year follow-ups, respectively, with a BED of ≤ 69.0 Gy. Contrary to the 3D-CRT results, poor local tumour control rates—and hence, low TCPs—were produced by the TCP model (see Fig. 3A, B, C, Table 1 and Table 2). The results obtained from the residuals analysis of the TCP model are summarised in Fig. 3D, 3E and 3F. This statistical test demonstrated that the TCP model yielded minimum and maximum residuals of 0.1% and −12%, respectively.

Fig. 4 displays the global minimum solution of the initial guess of the radio sensitivity components α and β and their standard deviations σ_α and σ_β, as produced by the NM simplex algorithm, for the 3D-CRT, CHART and SABR clinical outcome data for early-stage NSCLC.

3.2. Modelling clonogenic density decay in the GTV–CTV margins

Fig. 5 shows the results of the half-Gaussian clonogenic cell density decay and half-Gaussian dose-per-fraction decay in the GTV–CTV margins, with constant values for the clonogenic cell density and dose per fraction in the GTV for all of the 16 patient cohorts described in Table 1. For the region inside the GTV, all the graphs had a constant TCP inside the GTV, which was expected since both the clonogenic cell density and dose per fraction were constant. In the GTV–CTV margins, clonogenic cell density varied from 10^7 cm^{-3} to 10^0 cm^{-3} (see Fig. 5A). The dose per fraction was reduced to 40% of the maximum value for all cohorts (see Fig. 5B). Importantly, a relatively flat TCP was obtained in the GTV–CTV margin with a lower radiation dose, as displayed in Fig. 5C.

3.3. Modelling clonogenic density decay across the whole-tumour volume

Appendix 1 shows the results obtained using the approach described in Section 2.3.2, as applied to the 16 patient cohorts outlined in Table 1 and with a clonogenic cell density distribution and dose-per-fraction distribution of a half-Gaussian decay. Fig. 6 shows the results for four cohorts of patients: one 3D-CRT cohort, one CHART cohort and two SABR cohorts. It is immediately apparent that there is now a total of six graphs for each particular combination of cell density and dose distribution, corresponding to a graph for the dose-per-fraction profile, a graph for the clonogenic cell density profile, and separate graphs for each of the four patient cohorts. The dose per fraction was reduced to 40% of the maximum value for all cohorts, and clonogenic cell density varied from 1×10^7 cm^{-3} to 10^0 cm^{-3} at the outer edge of the treated volume. It is evident that values of high clonogenic cell density and low doses per fraction (the lower right side of Fig. 6C, D, E and F) produced poorly predicted TCP values. Likewise, for the values of low clonogenic cell density and high doses per fraction (the upper left side of Fig. 6C, D, E and F), the predicted TCP values were very high.

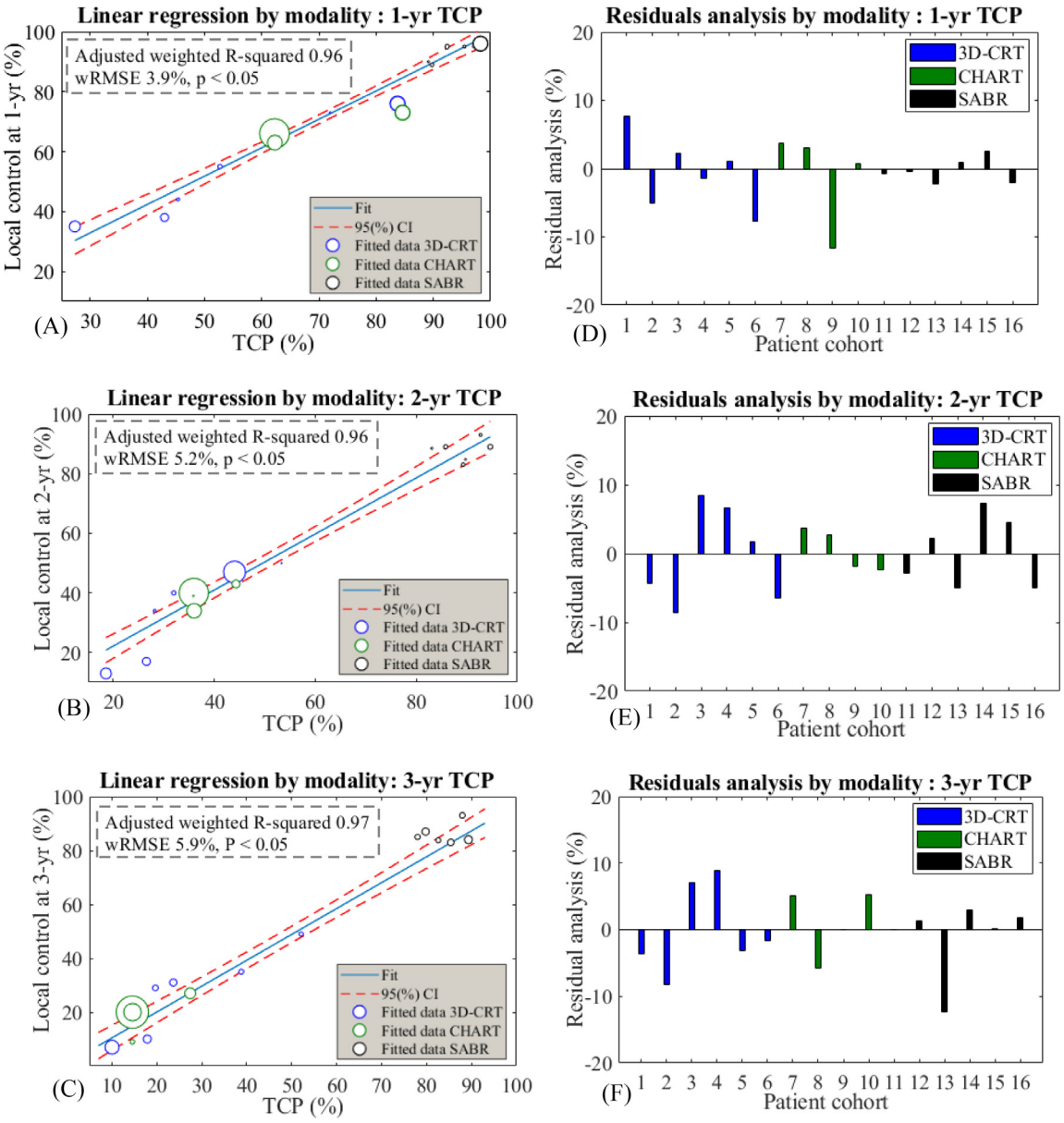

Fig. 3. Accuracy of the TCP models. The accuracy of TCP models was quantitatively assessed by employing a residuals analysis and determining the goodness of fit. Displayed here are the linear regression (A, B & C) graphs for 3D-CRT (green circles), CHART (blue circles) and SABR (black circles) radiotherapy, with 95% confidence bounds. Each dataset was statistically weighted and scaled based on the number of patients in each group.

3.4. Internal validation

Fig. 7 depicts the bootstrap results that were generated using 2000 bootstrap resamplings of the original dataset (training set). The histogram shows the variation of the correlation coefficients (Fig. 7A, B and C) and the RMSEs (Fig. 7D, E and F) across all of the bootstrap samples. The mean and the 95% confidence interval (CI) of the correlation coefficients (R^2) and the RMSEs of the local TCP in these 2000 samples with different clinical endpoints were as follows: one-year local tumour control, $R^2 = 0.98$ (95% CI = 0.93–0.99) and RMSE = 3.9 (95% CI = 2.6–6.3); two-year local tumour control, $R^2 = 0.98$ (95% CI = 0.95–0.99) and RMSE = 5.0 (95% CI = 4.0–6.3); and three-year local tumour control, $R^2 = 0.98$ (95% CI = 0.96–0.99) and RMSE = 5.5 (95% CI = 4.2–7.5).

4. Discussion

This study used clinical data from 16 published reports on early-stage NSCLC (see Table 1) to establish a TCP model. An LQ-based TCP model was found to provide an adequate estimate of local tumour control for early-stage NSCLC even though the LQ model's applicability in predicting local tumour control in hypofractionated radiotherapy regimens, such as SABR, has been a controversial and much-disputed subject within the field of radiobiology. Researchers have argued that SABR is characterised by markedly different radiobiology compared to conventional dose fractionation [15,16]. Moreover, a number of authors have argued that LQ-based TCP modelling underestimates SABR's local tumour control because it does not take into account collateral cell death and vascular damage [14,48]. High-dose radiotherapy directly damages DNA and produces simultaneous indirect effects, such as out-of-field tumour responses with abscopal and bystander effects. In these situations, antitumour immunity and immune-based tumour death can be triggered by cell signals, such as apoptosis, necrosis and necroptosis [49].

However, no reliable evidence has been provided to support any of these arguments. In fact, previous radiobiological modelling

Table 2
Summary of TCP predictions for one-year, two-year and three-year local tumour control rates.

RT modality	Patient cohorts	1-year TCP (%)	2-year TCP (%)	3-year TCP (%)
3D-CRT	1	29.5	18.2	11.1
3D-CRT	2	43.6	26.4	18.5
3D-CRT	3	52.9	32.0	24.0
3D-CRT	4	46.3	28.5	20.2
3D-CRT	5	70.1	44.7	37.5
3D-CRT	6	81.2	54.6	49.7
CHART	7	63.4	36.0	13.4
CHART	8	63.4	36.0	13.4
CHART	9	83.5	44.1	28.5
CHART	10	63.4	35.9	13.4
SABR	11	89.8	86.7	83.7
SABR	12	95.1	91.4	90.9
SABR	13	98.0	95.9	93.3
SABR	14	89.5	82.0	81.5
SABR	15	92.5	86.3	84.0
SABR	16	96.8	93.0	88.6

approaches [22,31,50], as well as the current study, have demonstrated that local tumour control in fractionated SABR of early-stage NSCLC is adequately modelled by extending the classic LQ formula to include the effects of hypoxia, tumour repopulation and the repair of sublethal damage. To the best of our knowledge, however, the present study is the first TCP model for early-stage NSCLC that has combined all three of these parameters. The TCP model used here accurately estimated local tumour control one, two and three years post-treatment for early-stage NSCLC patients who received either 3D-CRT, CHART or SABR. The model's statistical analysis expressed a strong positive linear relationship between the reported local tumour control and the predicted TCP outcomes. The model's results were strongly significant in both the fitted training datasets and the validated datasets (internal validation) and therefore provide a measure of confidence in the robustness of the current radiobiological models among the wide range of fractionation schemes and treatment modalities.

Some questions might be raised about the outcomes of the TCP model's statistical analysis. Is the dose escalation the main factor behind high local tumour control, or do other factors influence TCP, such as tumour size and patient selection? In patients with NSCLC, recent evidence has suggested that GTV is significantly associated with local tumour control [51]. For instance, Bradel et al. analysed 207 inoperable NSCLC patients treated with 3D-CRT to classify particular prognostic factors related to outcomes with 3D-CRT; their univariate and multivariate results indicated that GTV was the most significant factor for predicting local tumour control [52]. The study also raised the question of whether GTV size might be more crucial than the TNM staging system, which is the conventional approach for determining operability.

In another major study, 106 patients with newly diagnosed or recurrent stage I–III NSCLC were treated with 63–103 Gy in 2.1-Gy fractions, using 3D-CRT radiotherapy; the researchers found that tumour volume had no significant influence on local tumour control [34]. Moreover, when both the total radiation dose and GTV were incorporated into a Cox statistical analysis for local disease control and survival, only the total prescribed radiation doses were significant, and the treated tumour volume became less pronounced. This suggests that dose size is a more robust predictor for local tumour control than GTV. In the present study, the majority of the collected patient data was related to early-stage NSCLC; therefore, patient selection and tumour size were not the main reasons for the markedly different levels of local tumour control.

A number of published studies have described the efficacy of escalating radiation doses for medically inoperable early-stage NSCLC. These studies have suggested that higher radiation doses provide better local tumour control and increase overall survival. Both TCP and clinical outcomes (Fig. 2A, B, C, Table 1 and Table 2) have demonstrated that reducing the overall treatment time—typically an attempt to minimise the influence of the accelerated repopulation of cancer cells—played a crucial part in attaining an enhanced level of tumour control for NSCLC. However, increasing the treatment fractions may extend the total treatment time by more than three weeks, reaching the clonogen proliferation time zone and ultimately causing a loss of local tumour control [53]. Accordingly, CHART and SABR were superior to 3D-CRT in producing an improved level of TCP. Furthermore, fractionation schemes that were completed in fewer than 28 days showed only a small amount of repopulation, and the repopulation correction factor was therefore omitted for the subgroups of patients who received CHART or SABR. However, for treatment schemes that extended for more than 28 days, such as 3D-CRT, accelerated repopulation of the clonogenic cells is anticipated to occur for the remaining period of the treatment schedule, and this effect was therefore accounted for and modelled for the 3D-CRT data.

SABR is based on a philosophy that is distinct from other radiation therapy modalities because it utilises extremely high doses over just a few days (Table 1). It is considered standard in radiotherapy that delivering focused high doses of radiation destroys the maximum number of clonogenic cells and therefore achieves optimal TCP. However, the increased probability of complications in normal tissues restricts the use of high radiation doses. It is known that, in NSCLC, clonogenic cell density is lower at the periphery than in the centre of the GTV. However, previous studies of TCP models have not taken these variations into account, and few quantitative analyses have measured the actual number of clonogenic cells in NSCLC. To the best of our knowledge, only one study has attempted to measure the actual number of

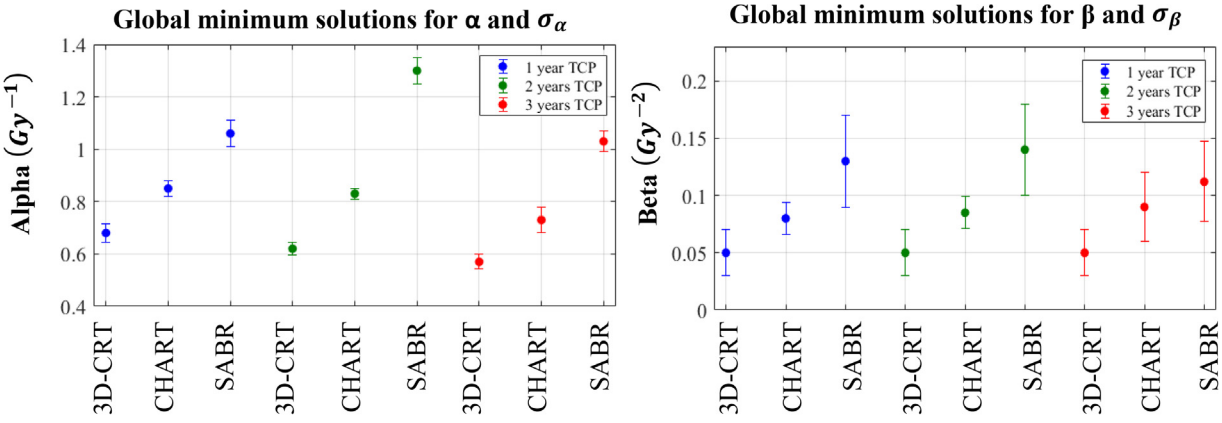

Fig. 4. The radiosensitivity solutions produced by the NM algorithm for each dataset. The error bars represent σ_α and σ_β.

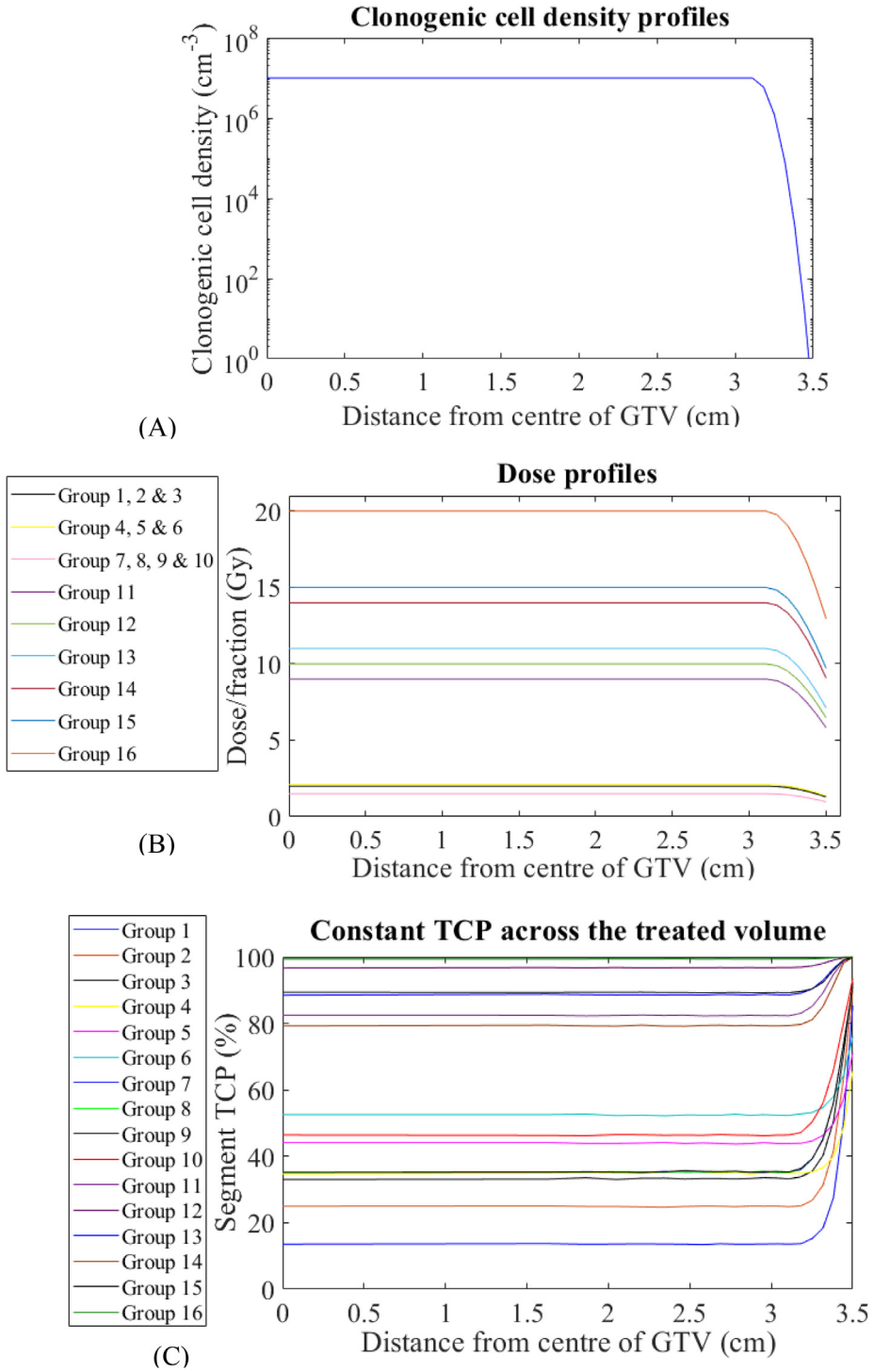

Fig. 5. Results of clonogenic cell density variations across a GTV–CTV margin of 5 mm. Both the dose per fraction (A) and clonogenic cell density (B) were constant throughout the GTV and fell off along a half-Gaussian decay across the GTV–CTV margin. A flat TCP was achieved across the treatment volume (C).

clonogens: that of Baker and Sanger [54], who attempted to determine the clonogenic cell density in human tumours and found it to be approximately $1.12 \times 10^5\,\mathrm{cm}^{-3}$.

The present study found that clonogenic cell density (see Fig. 5C) exhibited a spike towards 100% TCP at the very periphery of the CTV; this is because, by definition, the CTV should have a clonogenic cell density of 0 at its outer edge, with no clonogenic cells. This is a good indication that the processes of clonogenic cell density segmentation and dose distribution segmentation did not adversely affect the outcomes of the model. Moreover, the model indicated that there was a sigmoidal relationship between the dose per fraction and the predicted TCP (Fig. 6C, D, E and F). This can be considered a proof of concept, since it is consistent with the theory of Strigari et al. [55] that plotting the dose per fraction against the TCP is analogous to Fig. 6C, D, E and F, and it adds detail to the therapeutic index provided by Selvaraj et al. [56].

Accurate clinical outcome predictions can offer oncologists more reliable tools to enhance their decision making when balancing predicted benefits versus expected risk. As shown in this study, the established mechanistic TCP population model can sufficiently describe

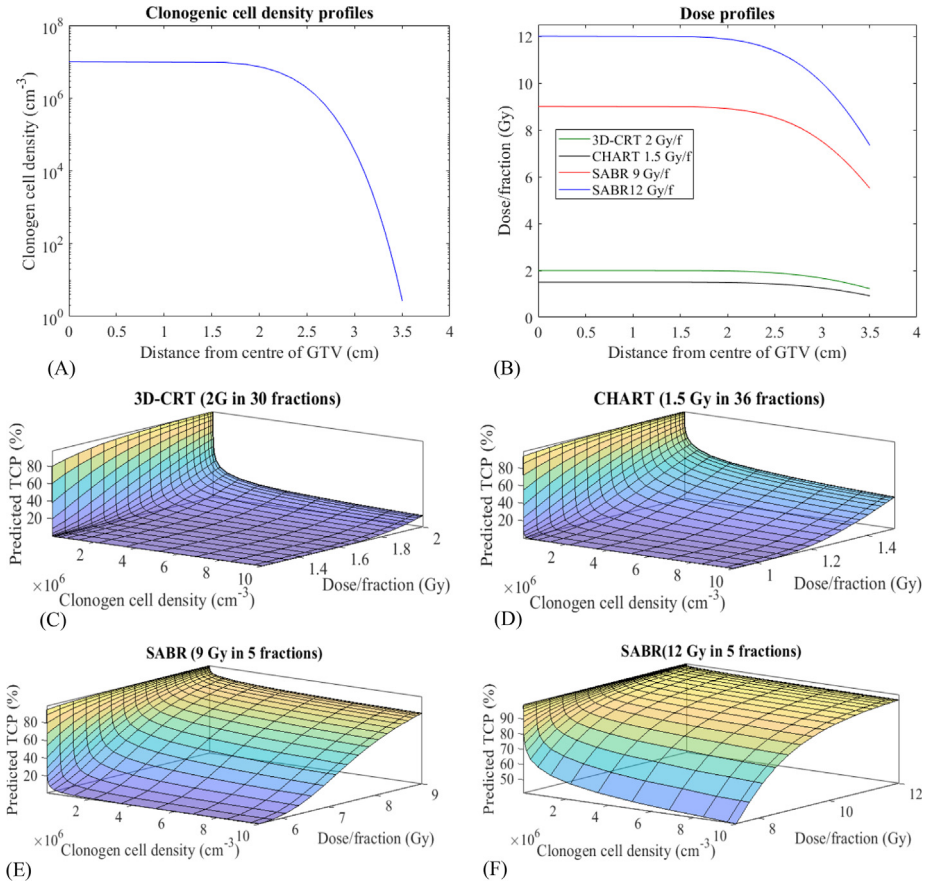

Fig. 6. Four cohorts of patients modelled in parallel for two years post local-control treatment. Both the dose per fraction and clonogenic cell density varied along a half-Gaussian decay.

the clinical outcomes of early-stage NSCLC. However, local tumour control is determined by a complicated interplay between radiation dosimetry, tumour biology, tumour microenvironment and patient-related variables. These factors present a challenge in establishing a prognostic model for routine clinical practice. Additionally, the TCP model has only been designed to predict population-level clinical outcomes, not individual-level clinical outcomes. Although the model could, theoretically, predict both individual- and population-level clinical outcomes, the precise voxel information for each individual (e.g., dose distribution, clonogenic distribution, intratumour radiosensitivity, etc.) would be required, and this is a significant limitation of TCP models.

Another major source of uncertainty in radiobiological modelling is associated with the accurate determination of the radiosensitivity parameters α, β, σ_α and σ_β. Data from several sources have shown high heterogeneity in reporting α and β values [57–61], indicating that α and β values can vary considerably between tumour sites and may even fluctuate between individuals. For NSCLC, a wide range of (α/β) values (2.2–12.6) has been reported in the literature [62–64]. Measurements of α, β, σ_α and σ_β can be performed *in vitro* in tumour cell lines or can be derived from clinical radiotherapy outcome data. In the current study, the radiosensitivity parameters were estimated by fitting the TCP to a broad spectrum of radiotherapy schedules using the NM simplex algorithm. The outcomes of the models showed that the actual values of (α/β) can vary from 7 to 14 depending on the radiotherapy modalities and, therefore, the fractionation schedules (Fig. 4).

Other factors believed to influence tumour response to radiation doses (such as cell cycling, tumour spatial heterogeneity, uncertainty associated with the delivery of radiation doses and interaction with the immune system) were not taken into account in this study. These variables play a vital role in determining clinical outcomes and remain a challenge to quantify and address with a modelling approach. Importantly, recent advances in radiotherapy (such as image-guided radiation therapy [IGRT], SABR, MRI-Linac and proton therapy) have improved the dosimetric uncertainties associated with treatment delivery [65–68]. However, such advances cannot entirely overcome the biological uncertainties. A good example of this is that the actual clonogenic density distribution of human tumours remains explicitly unknown, despite the tremendous recent developments in molecular imaging modalities. For instance, positron emission tomography (PET) resolution is limited to 5 mm[69]; microscopic diseases are considerably smaller than this, making the accurate determination of clonogenic density impossible. From a biological perspective, this issue remains one of the most significant gaps in the literature, and both physicists and radiobiologists, among other professionals in the radiation oncology community, must work together to resolve it.

5. Conclusion

This study sought to establish a mechanistic local TCP model that could describe clinical outcomes of early-stage NSCLC. The findings suggest that the TCP model is appropriate for the analysis and evaluation of radiotherapy treatment plans with respect to one-, two- and three-year local tumour control through 3D-CRT, CHART and SABR. The current study also shows that the TCP model can describe clinical outcomes at high doses per fraction, such as those used in SABR. The variations in clonogenic cell density, with respect to TCP, were investigated and modelled using a more practical approach to address a gap in the literature, which assumed that treated volume had a fixed clonogenic density.

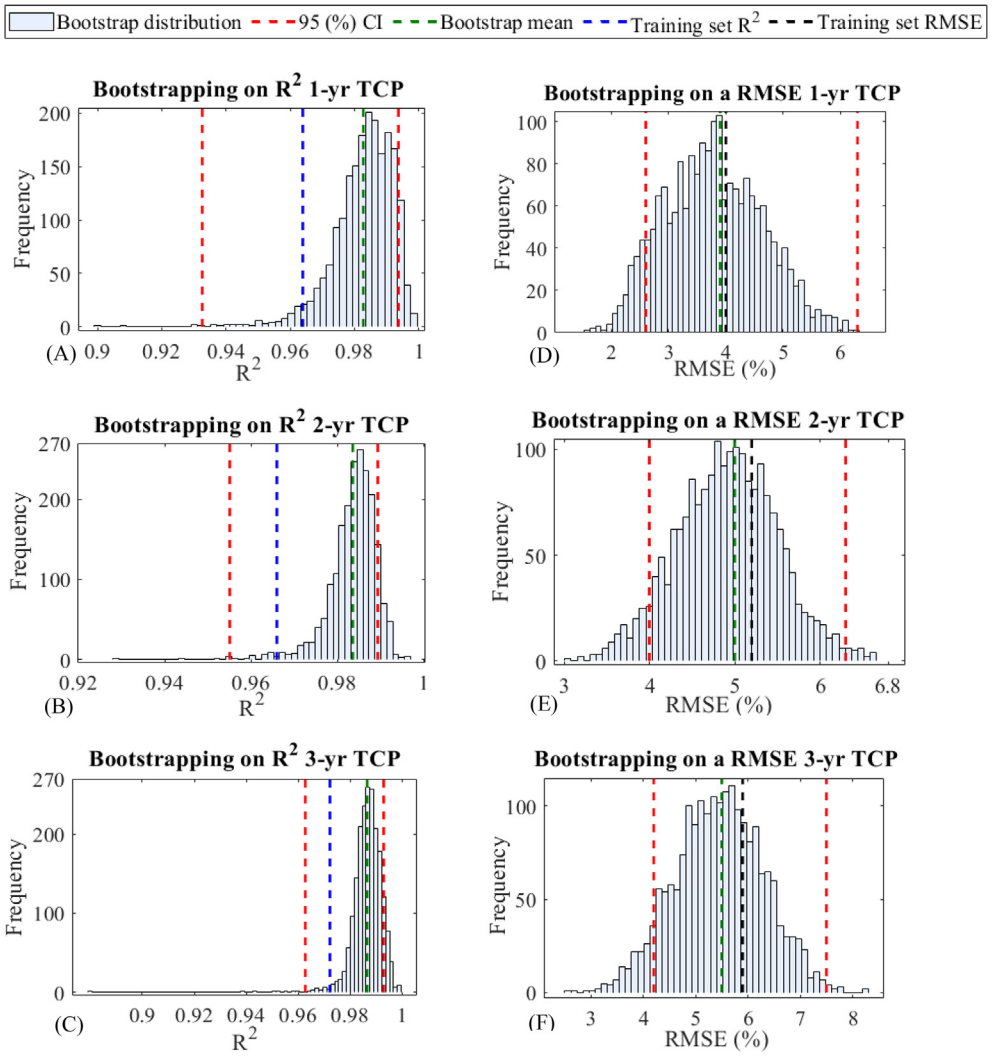

Fig. 7. Histogram of 2000 bootstrap samples on R^2 (A, B and C) and RMSE (D, E and F) for the one-, two- and three-year TCP model outcomes. These bootstrapping results were produced by resampling from the training set of 16 patient cohorts. The red broken vertical line indicates the boundaries of the bootstrap's 95% confidence interval, the green broken vertical line indicates the bootstrap sample mean, the blue broken vertical line indicates the R^2 value of the training set and the black broken vertical line indicates the RMSE value of the training set RMSE. The bootstrap histogram distribution of R^2 for all clinical endpoints is skewed to the left (negatively skewed histogram).

However, the present findings are subject to several complex radiobiological and physical limitations that must be taken into account. More clinical data are also required to externally validate and consolidate the model for robustness, accuracy and precision. These results, therefore, need to be interpreted with caution. A combination of chemotherapy and radiotherapy is a standard approach for locally advanced NSCLC that is perceived to offer superior local control. It would be interesting, therefore, to assess the effects of chemotherapy doses on overall TCP.

Declaration of Competing Interest

The authors declare that they have no known competing financial interests or personal relationships that could have appeared to influence the work reported in this paper.

Acknowledgements

The author wishes to acknowledge Dr Sean Walsh and Mr Morgan Healy for their help with MATLAB technical issues. The author would also like to thank the staff of National University of Ireland Galway and the Radiotherapy Department at University Hospital Galway for all of their assistance.

Funding

None.

Appendix A. Supplementary data

Supplementary data to this article can be found online at https://doi.org/10.1016/j.ejmp.2019.09.074.

References

[1] Ferlay J, Soerjomataram I, Dikshit R, Eser S, Mathers C, Rebelo M, et al. Cancer incidence and mortality worldwide: sources, methods and major patterns in GLOBOCAN 2012. Int J Cancer 2015;136:E359–86.
[2] Molina JR, Yang P, Cassivi SD, Schild SE, Adjei AA. Non-small cell lung cancer: epidemiology, risk factors, treatment, and survivorship. Mayo Clinic Proceedings: Elsevier; 2008. p. 584–94.
[3] Hatton MQF, Hill R, Fenwick JD, Morgan SA, Wilson PC, Atherton PJ, et al. Continuous hyperfractionated accelerated radiotherapy–Escalated dose (CHART-ED): a phase I study. Radiother Oncol 2016;118:471–7.
[4] Din OS, Harden SV, Hudson E, Mohammed N, Pemberton LS, Lester JF, et al. Accelerated hypo-fractionated radiotherapy for non small cell lung cancer: results from 4 UK centres. Radiother Oncol 2013;109:8–12.
[5] Taremi M, Hope A, Dahele M, Pearson S, Fung S, Purdie T, et al. Stereotactic body radiotherapy for medically inoperable lung cancer: prospective, single-center study of 108 consecutive patients. Int J Radiat Oncol Biol Phys 2012;82:967–73.
[6] Baumann M, Herrmann T, Koch R, Matthiessen W, Appold S, Wahlers B, et al. Final results of the randomized phase III CHARTWEL-trial (ARO 97-1) comparing hyperfractionated-accelerated versus conventionally fractionated radiotherapy in non-small cell lung cancer (NSCLC). Radiother Oncol 2011;100:76–85.
[7] Sanganalmath P, Lester J, Bradshaw A, Das T, Esler C, Roy A, et al. Continuous hyperfractionated accelerated radiotherapy (CHART) for non-small cell lung cancer

(NSCLC): 7 years' experience from nine UK centres. Clin Oncol 2018;30:144–50.
[8] Hamamoto Y, Kataoka M, Yamashita M, Nogami N, Sugawara Y, Kozuki T, et al. Factors affecting the local control of stereotactic body radiotherapy for lung tumors including primary lung cancer and metastatic lung tumors. Japanese J Radiol 2012;30:430–4.
[9] Andratschke N, Zimmermann F, Boehm E, Schill S, Schoenknecht C, Thamm R, et al. Stereotactic radiotherapy of histologically proven inoperable stage I non-small cell lung cancer: patterns of failure. Radiother Oncol 2011;101:245–9.
[10] Takeda A, Sanuki N, Kunieda E, Ohashi T, Oku Y, Takeda T, et al. Stereotactic body radiotherapy for primary lung cancer at a dose of 50 Gy total in five fractions to the periphery of the planning target volume calculated using a superposition algorithm. Int J Radiat Oncol Biol Phys 2009;73:442–8.
[11] Dunlap NE, Larner JM, Read PW, Kozower BD, Lau CL, Sheng K, et al. Size matters: a comparison of T1 and T2 peripheral non-small-cell lung cancers treated with stereotactic body radiation therapy (SBRT). J Thoracic Cardiovasc Surgery 2010;140:583–9.
[12] Kopek N, Paludan M, Petersen J, Hansen AT, Grau C, Høyer M. Co-morbidity index predicts for mortality after stereotactic body radiotherapy for medically inoperable early-stage non-small cell lung cancer. Radiother Oncol 2009;93:402–7.
[13] Brown W, Wu X, Fayad F, Fowler J, García S, Monterroso M, et al. Application of robotic stereotactic radiotherapy to peripheral stage I non-small cell lung cancer with curative intent. Clin Oncol 2009;21:623–31.
[14] Kirkpatrick JP, Meyer JJ, Marks LB. The linear-quadratic model is inappropriate to model high dose per fraction effects in radiosurgery. Seminars in Radiation Oncology: Elsevier; 2008. p. 240–3.
[15] Brown JM, Carlson DJ, Brenner DJ. The tumor radiobiology of SRS and SBRT: are more than the 5 Rs involved? Int J Radiat Oncol Biol Phys 2014;88:254–62.
[16] Fuks Z, Kolesnick R. Engaging the vascular component of the tumor response. Cancer Cell 2005;8:89–91.
[17] Kocher M, Treuer H, Voges J, Hoevels M, Sturm V, Müller R-P. Computer simulation of cytotoxic and vascular effects of radiosurgery in solid and necrotic brain metastases. Radiother Oncol 2000;54:149–56.
[18] Park HJ, Griffin RJ, Hui S, Levitt SH, Song CW. Radiation-induced vascular damage in tumors: implications of vascular damage in ablative hypofractionated radiotherapy (SBRT and SRS). Radiat Res 2012;177:311–27.
[19] Brenner DJ. The linear-quadratic model is an appropriate methodology for determining isoeffective doses at large doses per fraction. Seminars in Radiation Oncology: Elsevier; 2008. p. 234–9.
[20] Brown JM, Brenner DJ, Carlson DJ. Dose escalation, not "new biology", can account for the efficacy of stereotactic body radiation therapy with non-small cell lung cancer. Int J Radiat Oncol Biol Phys 2013;85:1159–60.
[21] Nahum AE, Movsas B, Horwitz EM, Stobbe CC, Chapman JD. Incorporating clinical measurements of hypoxia into tumor local control modeling of prostate cancer: implications for the α/β ratio. Int J Radiat Oncol Biol Phys 2003;57:391–401.
[22] Alaswad M, Kleefeld C, Moore M, Foley M. A TCP model for external beam treatment of non-small cell lung cancer. Phys Med 2018;52:172.
[23] Walsh S, Roelofs E, Kuess P, Lambin P, Jones B, Georg D, et al. A validated tumor control probability model based on a meta-analysis of low, intermediate, and high-risk prostate cancer patients treated by photon, proton, or carbon-ion radiotherapy. Med Phys 2016;43:734–47.
[24] Ruggieri R, Stavreva N, Naccarato S, Stavrev P. Computed 88% TCP dose for SBRT of NSCLC from tumour hypoxia modelling. Phys Med Biol 2013;58:4611.
[25] Ruggieri R, Naccarato S, Nahum AE. Severe hypofractionation: non-homogeneous tumour dose delivery can counteract tumour hypoxia. Acta Oncol 2010;49:1304–14.
[26] Baker C, Carver A, Nahum A. PO-0910: Local control prediction for NSCLC using a common LQ based TCP model for both SABR and 3D-CRT fractionation. Radiother Oncol 2015;115:S471.
[27] Stavreva N, Stavrev P, Balabanova A, Nahum A, Ruggieri R, Pressyanov D. Modelling the effect of spread in radiosensitivity parameters and repopulation rate on the probability of tumour control. Phys Med 2019;63:79–86.
[28] Giraud P, Antoine M, Larrouy A, Milleron B, Callard P, De Rycke Y, et al. Evaluation of microscopic tumor extension in non–small-cell lung cancer for three-dimensional conformal radiotherapy planning. Int J Radiat Oncol Biol Phys 2000;48:1015–24.
[29] Chao KC, Blanco AI, Dempsey JF. A conceptual model integrating spatial information to assess target volume coverage for IMRT treatment planning. Int J Radiat Oncol Biol Phys 2003;56:1438–49.
[30] Moher D, Liberati A, Tetzlaff J, Altman DG, Group P. Preferred reporting items for systematic reviews and meta-analyses: the PRISMA statement. 2010.
[31] Alaswad M, Kleefeld C, Foley M. Radiation dose intensity and local tumour control of non-small cell lung cancer: a radiobiological modelling perspective. J Phys: Conference Series: IOP Publishing 2019:012071.
[32] Saunders M, Dische S, Barrett A, Harvey A, Griffiths G, Parmar M. Continuous, hyperfractionated, accelerated radiotherapy (CHART) versus conventional radiotherapy in non-small cell lung cancer: mature data from the randomised multicentre trial. Radiother Oncol 1999;52:137–48.
[33] Lagerwaard FJ, Senan S, Van Meerbeeck JP, Graveland WJ, Group ROTS. Has 3-D conformal radiotherapy (3D CRT) improved the local tumour control for stage I non-small cell lung cancer? Radiother Oncol 2002;63:151–7.
[34] Kong F-M, Ten Haken RK, Schipper MJ, Sullivan MA, Chen M, Lopez C, et al. High-dose radiation improved local tumor control and overall survival in patients with inoperable/unresectable non–small-cell lung cancer: Long-term results of a radiation dose escalation study. Int J Radiat Oncol Biol Phys 2005;63:324–33.
[35] Ruggieri R, Stavrev P, Naccarato S, Stavreva N, Alongi F, Nahum AE. Optimal dose and fraction number in SBRT of lung tumours: a radiobiological analysis. Phys Med 2017;44:188–95.
[36] Thames HD. An 'incomplete-repair' model for survival after fractionated and continuous irradiations. Int J Radiat Biol Related Stud Phys Chem Med 1985;47:319–39.
[37] Mehta M, Scrimger R, Mackie R, Paliwal B, Chappell R, Fowler J. A new approach to dose escalation in non-small-cell lung cancer. Int J Radiat Oncol Biol Phys 2001;49:23–33.
[38] Griffin RJ. Int J Radiat Oncol Biol Phys 2006;66:627.
[39] Walsh S, Putten W. A TCP model for external beam treatment of intermediate-risk prostate cancer 2013.
[40] Nelder JA, Mead R. A simplex method for function minimization. Computer J 1965;7:308–13.
[41] Lind BK, Brahme A. The radiation response of heterogeneous tumors. Phys Med 2007;23:91–9.
[42] Nahum AE. The radiobiology of hypofractionation. Clin Oncol 2015;27:260–9.
[43] Park C, Papiez L, Zhang S, Story M, Timmerman RD. Universal survival curve and single fraction equivalent dose: useful tools in understanding potency of ablative radiotherapy. Int J Radiat Oncol Biol Phys 2008;70:847–52.
[44] Uzan J, Nahum A. Radiobiologically guided optimisation of the prescription dose and fractionation scheme in radiotherapy using BioSuite. Br. J. Radiol. 2012;85:1279–86.
[45] Webb S, Nahum A. A model for calculating tumour control probability in radiotherapy including the effects of inhomogeneous distributions of dose and clonogenic cell density. Phys Med Biol 1993;38:653.
[46] Brown JM, Diehn M, Loo Jr. BW. Stereotactic ablative radiotherapy should be combined with a hypoxic cell radiosensitizer. Int J Radiat Oncol Biol Phys 2010;78:323–7.
[47] Efron B. Bootstrap methods: another look at the jackknife. Breakthroughs in statistics: Springer; 1992. p. 569–93.
[48] Yamada Y, Bilsky MH, Lovelock DM, Venkatraman ES, Toner S, Johnson J, et al. High-dose, single-fraction image-guided intensity-modulated radiotherapy for metastatic spinal lesions. Int J Radiat Oncol Biol Phys 2008;71:484–90.
[49] Sologuren I, Rodríguez-Gallego C, Lara PC. Immune effects of high dose radiation treatment: implications of ionizing radiation on the development of bystander and abscopal effects. Transl. Cancer Res. 2014;3:18–31.
[50] Baker C, Carver A, Nahum A. Local control prediction for NSCLC using a common LQ-based TCP model for both SABR and 3D-CRT fractionation. Abstract at ESTRO 3rd Forum, Barcelona2015. p. 24–8.
[51] Chen M, Jiang G-L, Fu X-L, Wang L-J, Qian H, Zhao S, et al. Prognostic factors for local control in non-small-cell lung cancer treated with definitive radiation therapy. Am J Clin Oncol 2002;25:76–80.
[52] Bradley JD, Ieumwananonthachai N, Purdy JA, Wasserman TH, Lockett MA, Graham MV, et al. Gross tumor volume, critical prognostic factor in patients treated with three-dimensional conformal radiation therapy for non-small-cell lung carcinoma. Int J Radiat Oncol Biol Phys 2002;52:49–57.
[53] Fowler JF. Biological factors influencing optimum fractionation in radiation therapy. Acta Oncol 2001;40:712–7.
[54] Baker F, Sanger L. The density of clonogenic cells in human solid tumors. Int J Cell Cloning 1991;9:155–65.
[55] Strigari L, D'Andrea M, Abate A, Benassi M. A heterogeneous dose distribution in simultaneous integrated boost: the role of the clonogenic cell density on the tumor control probability. Phys Med Biol 2008;53:5257.
[56] Selvaraj JK. Modelling the effect of geometric uncertainties, clonogen distribution and IMRT interplay effect on tumour control probability. University of Liverpool; 2013.
[57] Pos FJ, Hart G, Schneider C, Sminia P. Radical radiotherapy for invasive bladder cancer: what dose and fractionation schedule to choose? Int J Radiat Oncol Biol Phys 2006;64.
[58] Qi XS, White J, Li XA. Is α/β for breast cancer really low? Radiother Oncol J Eur Soc Ther Radiol Oncol 2011:100.
[59] Datta NR, Rajkumar A, Basu R. Variations in clinical estimates of tumor volume regression parameters and time factor during external radiotherapy in cancer cervix: does it mimic the linear-quadratic model of cell survival? Indian J Cancer 2005;42.
[60] Williams SG, Taylor JMG, Liu N, Tra Y, Duchesne GM, Kestin LL. Use of individual fraction size data from 3756 patients to directly determine the alpha/beta ratio of prostate cancer. Int J Radiat Oncol Biol Phys 2007;68.
[61] Vernimmen FJAI, Slabbert JP. Assessment of the alpha/beta ratios for arteriovenous malformations, meningiomas, acoustic neuromas, and the optic chiasma. Int J Radiat Biol 2010;86.
[62] Van Leeuwen C, Oei A, Crezee J, Bel A, Franken N, Stalpers L, et al. The alfa and beta of tumours: a review of parameters of the linear-quadratic model, derived from clinical radiotherapy studies. Radiat Oncol 2018;13:96.
[63] Santiago A, Barczyk S, Jelen U, Engenhart-Cabillic R, Wittig A. Challenges in radiobiological modeling: can we decide between LQ and LQ-L models based on reviewed clinical NSCLC treatment outcome data? Radiat Oncol 2016;11.
[64] Stuschke M, Pottgen C. Altered fractionation schemes in radiotherapy. Front Radiat Ther Oncol 2010;42.
[65] Yamamoto T, Kabus S, Bal M, Bzdusek K, Keall PJ, Wright C, et al. Changes in regional ventilation during treatment and dosimetric advantages of CT ventilation image guided radiation therapy for locally advanced lung cancer. Int J Radiat Oncol Biol Phys 2018;102:1366–73.
[66] Bendall L, Papiez B, Hawkins M, Fenwick J. Isotoxic dose escalation with real-time imaging on an MR-linac in lung radiation therapy. Int J Radiat Oncol Biol Phys 2018;102:S207.
[67] Gomez DR, Li H, Chang JY. Proton therapy for early-stage non-small cell lung cancer (NSCLC). Transl Lung Cancer Res 2018;7:199.
[68] Astaraki M, Wang C, Buizza G, Toma-Dasu I, Lazzeroni M, Smedby Ö. Early survival prediction in non-small cell lung cancer from PET/CT images using an intra-tumor partitioning method. Phys Med 2019;60:58–65.
[69] Lazzeroni M, Uhrdin J, Carvalho S, van Elmpt W, Lambin P, Dasu A, et al. Evaluation of third treatment week as temporal window for assessing responsiveness on repeated FDG-PET-CT scans in Non-Small Cell Lung Cancer patients. Phys Med 2018;46:45–51.